

Thermal lens and heat generation of Nd:YAG lasers operating at 1.064 and 1.34 μm

C. Jacinto,¹ T. Catunda,² D. Jaque,³ L. E. Bausá,³ and J. García-Solé³

¹ Instituto de Física, Universidade Federal de Alagoas, 57072-970, Maceió, AL, Brazil

² Instituto de Física de São Carlos, Universidade de São Paulo, P.O. Box 369, São Carlos, SP, Brazil

³ Departamento de Física de Materiales, Universidad Autónoma de Madrid, Cantoblanco, 28049, Madrid, Spain

*Corresponding author: cjacinto@if.ufal.br

Abstract: We report on a simple and accurate method for determination of thermo-optical and spectroscopic parameters (thermal diffusivity, temperature coefficient of the optical path length change, pump and fluorescence quantum efficiencies, thermal loading, thermal lens focal length, etc) of relevance in the thermal lensing of end-pumped neodymium lasers operating at 1.06- and 1.3- μm channels. The comparison between thermal lensing observed in presence and absence of laser oscillation has been used to elucidate and evaluate the contribution of quantum efficiency and excited state absorption processes to the thermal loading of Nd:YAG lasers.

©2008 Optical Society of America

OCIS codes: (140.6810) Thermal effects; (160.3380) Laser materials; (160.4760) Optical properties.

References and links

1. W. Koehner, *Solid-State Laser engineering* (Springer - Verlag, New York, 1988).
2. A. A. Kaminskii, *Laser Crystals*, 2nd ed. (Springer, Berlin, 1990).
3. T. Y. Fan, "Heat-Generation in Nd:YAG and Yb:YAG," *IEEE J. Quantum Electron.* **29**, 1457-1459 (1993).
4. J. L. Blows, T. Omatsu, J. Dawes, H. Pask, and M. Tateda, "Heat generation in Nd:YVO₄ with and without laser action," *IEEE Photon. Technol. Lett.* **10**, 1727-1729 (1998).
5. C. Jacinto, S. L. Oliveira, T. Catunda, A. A. Andrade, J. D. Myers, and M. J. Myers, "Upconversion effect on fluorescence quantum efficiency and heat generation in Nd³⁺-doped materials", *Opt. Express* **13**, 2040-2046 (2005); <http://www.opticsinfobase.org/abstract.cfm?URI=oe-13-6-2040>
6. M. Okida, M. Itoh, T. Yatagi, H. Ogilvy, J. Piper, and T. Omatsu, "Heat generation in Nd doped vanadate crystals with 1.34 μm laser action," *Opt. Express* **13**, 4909-4915 (2005); <http://www.opticsinfobase.org/abstract.cfm?URI=oe-13-13-4909>.
7. B. Neuenschwander, R. Weber, and H. P. Weber, "Determination of the thermal lens in solid-state lasers with stable cavities," *IEEE J. Quantum Electron.* **31**, 1082-1087 (1995).
8. B. Ozygus and Q. C. Zhang, "Thermal lens determination of end-pumped solid-state lasers using primary degeneration modes," *Appl. Phys. Lett.* **71**, 2590-2592 (1997).
9. M. Montes, D. Jaque, Z. D. Luo, and Y. D. Huang, "Short-pulse generation from a resonantly pumped NdAl₃(BO₃)₄ microchip laser," *Opt. Lett.* **30**, 397-399 (2005).
10. S. Fan, X. Zhang, Q. Wang, S. Li, S. Ding, and F. Su, "More precise determination of thermal lens focal length for end-pumped solid-state lasers," *Opt. Commun.* **266**, 620-626 (2006).
11. C. Jacinto, D. N. Messias, A. A. Andrade, S. M. Lima, M. L. Baesso, and T. Catunda, "Thermal lens and Z-scan measurements: Thermal and optical properties of laser glasses - A review", *J. Non-Cryst. Solids* **352**, 3582-3597 (2006).
12. M. L. Baesso, J. Shen, and R. D. Snook, "Mode-mismatched thermal lens determination of temperature coefficient of optical path length in soda lime glass at different wavelengths", *J. Appl. Phys.* **75**, 3732-3737 (1994).
13. M. E. Innocenzi, H. T. Yura, C. L. Fincher, and R. A. Fields, "Thermal modeling of continuous-wave end-pumped solid-state lasers," *Appl. Phys. Lett.* **56**, 1831-1833 (1990).
14. C. Jacinto, A. A. Andrade, T. Catunda, S. M. Lima, and M. L. Baesso, "Thermal lens spectroscopy of Nd:YAG," *Appl. Phys. Lett.* **86**, 034104 (2005).
15. J. Shen, R. D. Lowe, and R. D. Snook, "A model for cw laser induce mode-mismatched dual-beam thermal lens spectrometry", *Chem. Phys.* **165**, 385-396 (1992).

16. D. C. Brown, "Heat, fluorescence, and stimulated-emission power densities and fractions in Nd:YAG," *IEEE J. Quantum Electron.* **34**, 560-572 (1998).
17. S. Küick, L. Fornasiero, E. Mix, and G. Huber, "Excited state absorption and stimulated emission of Nd³⁺ in crystals. Part I: Y₃Al₅O₁₂, YAlO₃, and Y₂O₃," *Appl. Phys. B-Lasers and Optics* **67**, 151-156 (1998).
18. Y. Guyot, H. Manaa, J. Y. Rivoire, R. Moncorge, N. Garnier, E. Descroix, M. Bon, and P. Laporte, "Excited-state-absorption and up-conversion studies of Nd³⁺-doped single crystals Y₃Al₅O₁₂, YLiF₄, and LaMgAl₁₁O₁₉," *Phys. Rev. B* **51**, 784-799 (1995).
19. N. Pavel, V. Lupei, J. Saikawa, T. Taira, and H. Kan, "Neodymium concentration dependence of 0.94-, 1.06- and 1.34- μm laser emission and of heating effects under 809- and 885- nm diode laser pumping of Nd:YAG," *Appl. Phys. B-Lasers and Optics* **82**, 599-605 (2006).
20. R. C. Powell, *Physics of Solid-State Laser Materials* (Springer, New York, 1998).

1. Introduction

Pump and laser induced Thermal Lens (TL) is a crucial effect in laser materials, especially when operating in an end-pumping configuration (due to the much localized heat deposition achieved in this case). In most of the situations TL is an undesirable effect that leads to deterioration in the laser output power and/or in the spatial quality of the laser beam. On the other hand, in some configurations, such as microchip designs, TL is required for stable laser oscillation. In any case, and independently of the geometrical configuration of the laser cavity used, a precise knowledge of the thermo-optical and spectroscopic properties of the system, determining the generated heat in the active volume and the induced TL, is very important to laser design [1,2]. Some properties, particularly the TL dioptric power ($D_{\text{TL}}=f_{\text{TL}}^{-1}$) and thermal loading, change when the system is under laser action [3,4]. Furthermore, in some cases the presence of excited state absorption (ESA) and/or Auger upconversion at laser wavelength could lead to the appearance of additional heating sources different to those associated to pump radiation [5,6]. Thus, it is very important for an accurate determination of these properties, the realization of the measurements with the system in real conditions of functionality, i.e., in the presence of laser oscillation.

The quantitative determination of the effective focal length due to thermal effects in end-pumped lasers is difficult compared to lamp-pumped due to the small size involved and also due to the higher sensitivity required. Several different approaches have been used including those based on interferometry, analysis of the output beam parameters, transverse mode beat frequency, and degeneration in the resonator length [7-10]. Nevertheless, most of these methods are inaccurate and some important features are not well understood. For instance, it is recognized that the end-face curvature of the sample should contribute to TL due to the hotter center of the sample compared to its edge (the surface bulging effect) [11,12]. However, this effect is not well quantitatively known and most papers consider only the temperature coefficient of the refractive index (dn/dT) to estimate D_{TL} [8,13]. Moreover, how crystal defects affect the pumping and fluorescence efficiencies and, consequently, the heat generation is still uncertain. Although these subjects have been extensively studied, they have proven to be quite difficult with many conflicting results in the literature [14].

The dual-beam mode-mismatched TL spectrometry (MMTLS) was developed to improve the sensitivity of TL measurements [15]. It is a simple, accurate, and very sensitive method for the determination of TL induced phase-shifts (up to $\sim\lambda/10^8$) and thermo-optical properties. It has been successfully applied to laser materials for accurate determination of thermal diffusivity, temperature coefficient of the optical path change (ds/dT), fluorescence quantum efficiency (η), and Auger upconversion parameter [11]. In this work, the MMTLS was applied to an intracavity experiment, a diode end-pumped Nd:YAG laser oscillating at 1.064 and 1.34 μm . Most of previous papers [4,6-9] used TL only to measure D_{TL} while the fractional thermal loading (the rate of heat generated to absorbed energy) and quantum efficiency were determined by other photothermal methods or estimated from lifetime measurements and Judd-Ofelt calculations [3,6]. In this paper, we demonstrated that the analysis of laser and TL data (without and with laser oscillation at 1.064 and 1.34 μm) allows a precise determination of several important laser and spectroscopic parameters: D_{TL} , the pump efficiency (at 808nm), the fractional thermal loading (ϕ), and the effect of ESA on ϕ at 1.34 μm .

2. Theoretical background and experiment

In the MMTLS experiment, a probe laser beam crosses the pumped volume of the sample and consequently a change in its on-axis intensity takes place, which in the far-field is given by [15]:

$$I(t) = I(0) \left\{ 1 - \frac{\theta}{2} \operatorname{atan} \left[\frac{2 m V}{\left[(1+2 m)^2 + V^2 \right] t_c / 2 t + 1 + 2 m + V^2} \right] \right\}^2 \quad (1)$$

Where $m = (w_p/w_{ex})^2$, $V = Z_l/Z_c$ (when $Z_c \ll Z_l$), Z_c is the confocal distance of the probe beam, Z_l is the distance between the probe beam waist and the sample, Z_2 is the distance between the sample and the photodiode, w_p and w_{ex} are the probe and excitation beams radii at the sample position, respectively, $I(0) = I(t)$ when the transient time t or θ is zero, t_c is the characteristic TL signal time, which is related to the thermal diffusivity by $D = w_{ex}^2/4t_c$, and this one to the thermal conductivity by $K = \rho c D$, where ρ is the density and c the specific heat. θ is approximately the phase difference of the probe beam at $r = 0$ and $r = \sqrt{2} w_{ex}$ induced by TL, which is given by [11,12,14,15]:

$$\theta = -\frac{P_{abs}}{\lambda_p K} \left(\frac{ds}{dT} \right) \varphi \quad (2)$$

where λ_p is the probe beam wavelength, P_{abs} is the absorbed pump power, and φ is the fraction of absorbed energy converted into heat (also called fractional thermal loading). Since the fluorescence quantum efficiency of higher-lying levels than the metastable state (${}^4F_{3/2}$) is negligible, Nd:YAG can be considered as presenting only one emitting state. In this case, φ is given by [3,6,11,14]:

$$\varphi = 1 - \eta_p \left[(1 - \eta_l) \eta_f \frac{\lambda_{ex}}{\langle \lambda_{em} \rangle} + \eta_l \frac{\lambda_{ex}}{\lambda_l} \frac{1}{1 + \sigma_{ESA} / \sigma_{SE}} \right] \quad (3)$$

where $\eta_p \approx 1$ is the pump quantum efficiency (the fraction of absorbed pumping photons contributing to inversion), η_f is the fluorescence quantum efficiency, η_l is the laser extraction efficiency (the fraction of excited ions that are extracted by stimulated emission), λ_l is the laser wavelength. In the case of diode pumped Nd:YAG crystals the excitation wavelength (λ_{ex}) and the average emission wavelength ($\langle \lambda_{em} \rangle$) are 808 and 1050 nm, respectively. In expression (3) σ_{SE} is the stimulated emission cross-section and σ_{ESA} is the ESA cross-section at the laser action wavelength. Self-absorption of the fluorescence was not taken into account in Eq. (3) because absorption at the emission wavelengths of Nd:YAG are negligible. From the knowledge of the TL-induced phase shift (θ), it is possible to obtain the dioptric power [13,14]:

$$D_{TL} = -\frac{\lambda_p \theta}{\pi w_{ex}^2} = \frac{P_{abs}}{\pi w_{ex}^2 K} \left(\frac{ds}{dT} \right) \varphi = C \varphi P_{abs} \quad (4)$$

in which $C = (\pi w_{ex}^2 K)^{-1} ds/dT$ is a constant that depends on thermo-optical properties of the sample. The parameter θ is obtained from the fit of TL transient signal, as detailed elsewhere [11,12,14,15]. According to Eq. (4), the product $C\varphi$ can be achieved from the plot of D_{TL} (calculated from θ) versus P_{abs} .

The experimental setup used in this work is shown in Fig. 1. It is similar to that used in previous works concerning MMTLS with the only difference that in this case the crystal under study was placed in a laser cavity. The laser cavity was composed of an input mirror with 10 cm radius of curvature and a flat output coupler. Both mirrors were highly-transmitting (HT) at the pump wavelength and highly-reflecting (HR) at the laser wavelength. The pump source was a fiber coupled LIMO laser diode operating at 808 nm, with TM_{00} mode, and quality factor $M^2 = 3.5$. The fiber has 100 μm diameter, a numeric aperture of 0.22, and a bandwidth of 1 nm. Before focusing, the laser radiation was collimated by an OFCR

adjustable fiber collimator. The probe beam was a He-Ne laser operating at 632.8 nm. The detection system consisted of a Si detector, a digital oscilloscope, and a computer. The pump and probe beams were nearly counter-propagating in a small angle ($<1.5^\circ$), in order to deviate the probe beam to photodiode detector positioned in the far field. It was already demonstrated that this small angle does not affect the TL signal [12,14]. To maximize the signal, the probe beam was aligned to pass through the center of TL induced by the excitation beam. The investigated sample was a Nd:YAG commercial crystal (Cstech Inc.) with a nominal Nd^{3+} concentration of 1.0 at.% and size of $1.5 \times 2.5 \times 3.0 \text{ mm}^3$ with the optical path along the shortest thickness (the absorption coefficient at 808.6nm is $\sim 9.5 \text{ cm}^{-1}$).

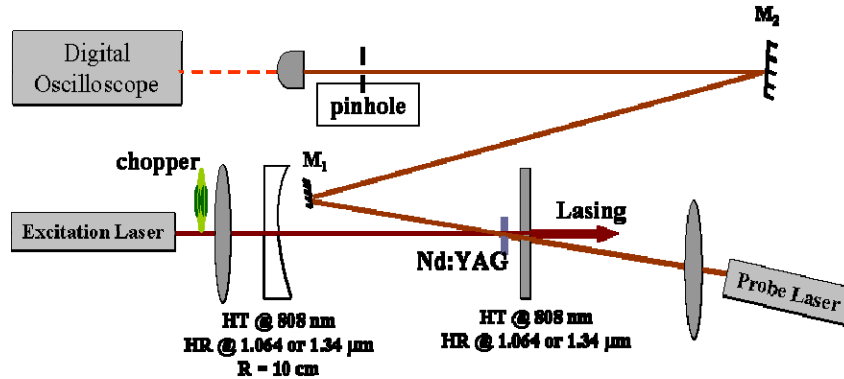


Fig. 1. Experimental setup for thermal lens experiments intra-cavity.

3. Results and discussion

Figure 2 shows typical TL transients obtained from the Nd:YAG samples with (at $1.064 \mu\text{m}$) and without laser action for $P_{\text{abs}} = 0.44$ and 0.40 W , respectively. The smaller amplitude of the TL signal with laser oscillation is an indication of reduced heat generation. From the fitting with Eq. (1), it was obtained $\theta_{\text{no-lasing}} = -(194.5 \pm 0.2) \times 10^{-3} \text{ rad}$, $\theta_{\text{lasing}} = -(162.8 \pm 0.2) \times 10^{-3} \text{ rad}$, and for the two transients $t_c = (160 \pm 6) \mu\text{s}$. From this t_c and $w_{\text{ex}} = 55 \mu\text{m}$, $D = (47 \pm 2) \times 10^{-3} \text{ cm}^2/\text{s}$ was obtained, in agreement with the expected value for Nd:YAG crystal [1,2,14,16].

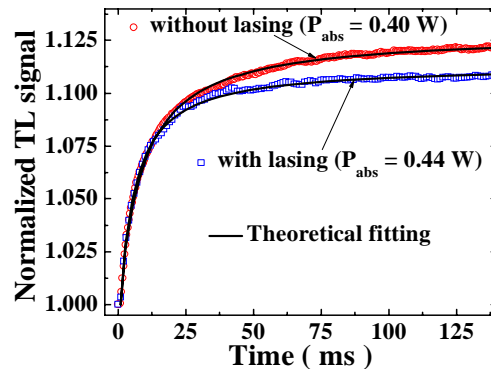


Fig. 2. Normalized TL signal from Nd:YAG crystal with (at $1.064 \mu\text{m}$) and without laser action. The absorbed pump powers were 0.40 and 0.44 W for no-lasing and lasing conditions, respectively.

The measured laser curve and D_{TL} versus P_{abs} without and with laser operation at $1.064 \mu\text{m}$ is shown in Fig. 3 (a). The data are very well fit by straight lines with a clear distinction between before and after laser threshold. This indicates that an abrupt transition from $\eta_l = 0$ (no lasing condition) to $\eta_l \approx 1$ (under lasing operation) takes place [Eqs. (3) and (4)]. The correspondents $C\phi$ parameters obtained from the linear fit of Fig. 3 (a) data were

$C\varphi_{\text{no lasing}} = (32.2 \pm 0.4) \text{ m}^{-1}/\text{W}$ and $C\varphi_{\text{lasing}}^{1.06} = (25.3 \pm 0.7) \text{ m}^{-1}/\text{W}$. So, 1.064 μm laser action reduces the thermal load by $\sim 21\%$ as predicted by Brown [16]. In order to interpret these results, several spectroscopic features of Nd:YAG have to be considered. A nonunity η_p would account for nonunity transfer efficiency from pump to metastable level or dead sites [3]. In some Nd:YAG crystals, a broad absorption band can be noticed in the visible indicating color centers or some defects [3,14,20]. However, in the near infrared range (730 – 900 nm) an overall coincidence is observed between the absorption, excitation, and photothermal spectra, which present only the characteristic of Nd^{3+} line sharps [14]. Then, $\eta_p \approx 1$ can be assumed for excitation at 808nm. By a simple inspection of the energy level diagram of the Nd:YAG system, ESA at 1.064 μm should be negligible. Therefore, we can assume $\sigma_{\text{ESA}}/\sigma_{\text{SE}} \approx 0$ in Eq. (3). This assumption is not only supported by previous spectroscopic works [17,18], but also by the absence of any additional visible luminescence (upconversion) originated from higher energy levels in laser-on conditions. Comparing the values with and without laser action by means of the following equation:

$$\frac{D_{\text{TL}}^{\text{no lasing}}}{D_{\text{TL}}^{\text{lasing}}} = \frac{\varphi_{\text{no lasing}}}{\varphi_{\text{lasing}}} = \frac{1 - \eta_f \lambda_{\text{ex}} / \langle \lambda_{\text{em}} \rangle}{1 - \lambda_{\text{ex}} / \lambda_l} \quad (5)$$

the fluorescence quantum efficiency $\eta_f = (0.90 \pm 0.03)$ was obtained. Using this η_f value in $C\varphi_{\text{no lasing}} = (32.2 \pm 0.4) \text{ m}^{-1}/\text{W}$ [Eq. (3) with $\eta_l = 0$], $C = (105 \pm 5) \text{ m}^{-1}/\text{W}$ was calculated. Since $C = (\pi w_{\text{ex}}^2 K)^{-1} ds/dT$, with $K = 13 \text{ W/mK}$ and $w_{\text{ex}} = 55 \mu\text{m}$, we have found $ds/dT = (13.0 \pm 0.7) \times 10^{-6} \text{ K}^{-1}$. These η_f and ds/dT values are in good agreement with those previously determined for 0.75 at.% doped Nd:YAG crystal using multiwavelength TL spectroscopy, $\eta_f = (0.95 \pm 0.02)$ and $ds/dT = (13.7 \pm 0.9) \times 10^{-6} \text{ K}^{-1}$ [14].

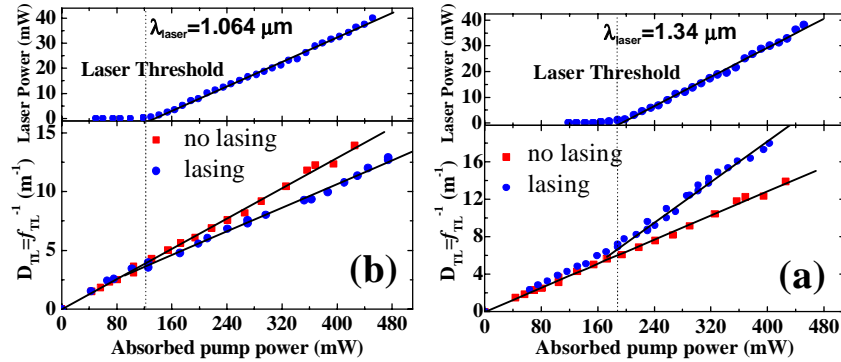


Fig. 3. (a) Laser emission at 1.064 μm (top), TL dioptric power (bottom) with (circles) and without (squares) lasing at 1.064 μm ; (b) Laser emission at 1.34 μm (top), and TL dioptric power (bottom) with (circles) and without (squares) lasing at 1.34 μm as a function of the absorbed pump power for Nd:YAG doped with 1.0 at.%.

Most papers on TL in end-pumped solid-state lasers analyze their results considering in Eq. (4) only dn/dT instead of ds/dT , as modeled by Innocenzi *et al* [13]. However, Neuenschwander *et al* [7] observed a TL focal length 30% smaller (or larger D_{TL}) than that predicted using dn/dT and attributed this difference to the surface bending (bulging), stress, and strain induced refractive index change. All these effects can be taken into account replacing dn/dT by an effective ds/dT [12,14] (note that $D_{\text{TL}} \propto ds/dT$ by Eq. (4)). An approximated simple analytical expression is available for two geometries: disk ($L \ll D_d$) and rod ($L \gg D_d$), where L and D_d represent the cylinder length and diameter, respectively. In the case of Nd:YAG, ds/dT is larger than dn/dT by a factor of 1.3 and 2.2 for rod and disk geometry, respectively [1,14]. Neuenschwander *et al.* [7] obtained a factor 1.3 as expected for

rod geometry (in their experiment $L \approx 4D_d$). We obtained a factor 1.8 (lower than 2.2) probably because our sample is not thin enough, $L \approx D_d/2$.

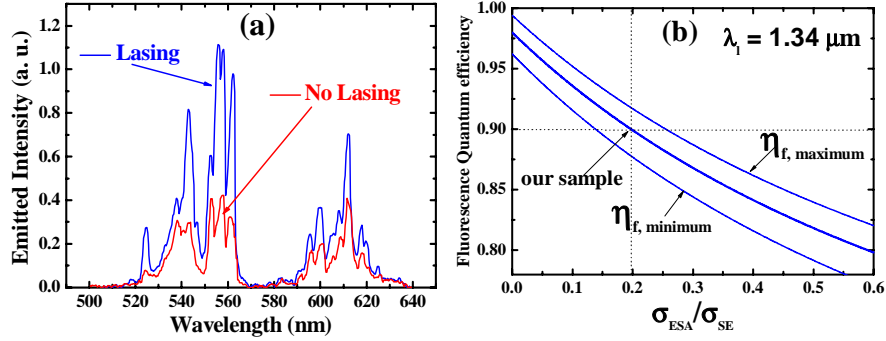


Fig. 4. (a) Visible luminescence spectra of the Nd:YAG crystal in the presence and absence of laser oscillation at 1.34 μm . The absorbed pump power was 0.40 W. (b) Fluorescence quantum efficiency versus $\sigma_{\text{ESA}}/\sigma_{\text{SE}}$ obtained from the $\varphi_{\text{lasing}}^{1.34\mu\text{m}}$ and $\varphi_{\text{no lasing}}$ data using Eq. (3).

The discussion about η_f will be made after the analysis of the data obtained for 1.34 μm laser action shown in Fig. 3 (b). At variance with the case of laser action at 1.064 μm (Fig. 3 (a)), the thermal loading is increased in the presence of laser oscillation. In fact, $C\varphi_{\text{lasing}}^{1.34} = (52 \pm 2) \text{ m}^{-1}/\text{W}$, which is twice larger than that with laser operation at 1.064 μm and 62% larger than without laser action. A similar increase of thermal load ($\sim 2\times$) was observed in Nd doped YAG and vanadate crystals [6,19], when compared 1.064 and 1.34 μm laser oscillation. There are several reasons for the higher thermal loading observed for 1.34 μm laser operation. Firstly, the higher quantum defect due to the longer laser wavelength. Secondly, we have observed a strong green luminescence originated from the active volume when laser oscillation is achieved (see Fig. 4 (a)). This 1.34 μm laser induced visible fluorescence has been attributed to ESA of laser radiation resulting in a population of the ${}^4\text{G}_{7/2}$ state (Auger upconversion is less possible, given the doping levels of the studied sample [4,5,18]). Consequently the assumption $\sigma_{\text{ESA}}/\sigma_{\text{SE}} \approx 0$, made for the case of 1.064 μm laser operation, is not longer valid for analysis of the 1.34 μm laser oscillation data. The effect of σ_{ESA} is equivalent to increase the quantum defect since λ_l is multiplied by the factor $(1 + \sigma_{\text{ESA}}/\sigma_{\text{SE}})$. Substituting the experimental data of $\varphi_{\text{lasing}}^{1.34}/\varphi_{\text{lasing}}^{1.06}$ in Eq. (3), the value $\sigma_{\text{ESA}}/\sigma_{\text{SE}} = 0.19 \pm 0.02$ is obtained in good agreement with $\sigma_{\text{ESA}}/\sigma_{\text{SE}} \approx 0.14$ (at $\sim 1.34 \mu\text{m}$, $\sigma_{\text{ESA}} \approx 8 \times 10^{-21} \text{ cm}^2$ and $\sigma_{\text{SE}} \approx 5.8 \times 10^{-20} \text{ cm}^2$) estimated from ESA data, which are not very accurate (ESA experiment presents serious problems of calibration) [17,18]. Then, using $\sigma_{\text{ESA}}/\sigma_{\text{SE}} = 0.19 \pm 0.02$ and the data of $\varphi_{\text{lasing}}^{1.34}/\varphi_{\text{no lasing}}$ we obtained $\eta_f = 0.90 \pm 0.04$, corroborating the η_f value previously calculated from $\varphi_{\text{lasing}}^{1.064}/\varphi_{\text{no lasing}}$. Alternatively, we could use $\varphi_{\text{lasing}}^{1.34}/\varphi_{\text{no lasing}}$ data assuming $\sigma_{\text{ESA}}/\sigma_{\text{SE}} \approx 0.14$ (from ESA data) to obtain $\eta_f = 0.92$, in agreement with the previous value. According to this procedure, Fig. 4 (b) simulates the effect of $\sigma_{\text{ESA}}/\sigma_{\text{SE}}$ on η_f , calculated from $\varphi_{\text{lasing}}^{1.34\mu\text{m}}$ and $\varphi_{\text{no lasing}}$ data using Eq. (3). The effect of η_p was also investigated and indicates that decreasing the value of η_p and/or η_f implies in $\sigma_{\text{ESA}}/\sigma_{\text{SE}}$ much higher than 0.2, which is in contradiction with ESA data at 1.34 μm . For instance, using $\eta_p = 0.90$ with $\varphi_{\text{lasing}}^{1.064}/\varphi_{\text{no lasing}}$ data we obtain $\eta_f = 0.86$ and $\sigma_{\text{ESA}}/\sigma_{\text{SE}} = 0.57$. Thus, we concluded that our data corroborate the assumption of unitary η_p for excitation at 808nm and $\eta_f = 0.90$ ($\varphi_{\text{no lasing}} = 0.30$). Our results are also consistent with $\varphi_{\text{no lasing}} = 0.27$ and $\eta_f = 0.95$ obtained by TL in a 0.75 at.% doped Nd:YAG crystal [14]. Both results are in agreement with the calculated $\eta_{\text{cal}} = \tau_{\text{exp}}/\tau_{\text{rad}}$. From Judd-Ofelt analysis it is expected $\tau_{\text{rad}} \approx 259 \mu\text{s}$ in excellent

agreement with lifetime measurements of diluted crystal ($\tau_{\text{exp}} \approx 260\mu\text{s}$), since multiphonon decay should have negligible effect. Due to cross relaxation ion-ion interaction τ_{exp} decrease with Nd^{3+} concentration and for ≈ 1 at.% doped Nd:YAG crystals it is expected $\eta_{\text{cal}} \approx 0.9$ [2,20]. However, it should be noticed that η_p might depend on crystal preparation procedures since nonunitary pump efficiency is usually attributed to defects or impurities [3,14,20].

4. Conclusion

In summary, we have applied the MMTLS to analyze the pump and laser induced thermal lensing of Nd:YAG crystals operating at 1.064 and 1.34 μm laser channels. This method is characterized by its simplicity, sensitivity, and accuracy, providing information about TL and other physical properties. We obtained fractional thermal loadings of ≈ 0.30 , 0.24, and 0.49 for the cases of no lasing, laser oscillation at 1.06, and laser oscillation at 1.34 μm , respectively. We conclude that for excitation at 808 nm, the pumping efficiency is close to unity and the fluorescence quantum efficiency is ≈ 0.90 . We have found that ESA plays no role for 1.064 μm laser oscillation but for 1.34 μm laser it increases the fractional thermal loading by $\approx 23\%$. Besides, the TL results evidenced the importance of the end-face curvature or bulging effect ($ds/dT \approx 1.8 \times dn/dT$) in the TL created in Nd:YAG lasers. It is worth noting that, all these parameters were obtained with the system in real laser action, differently from previous TL experiments [5, 11, 14]. All experimental data (with and without laser action) could be described by a simple theoretical model that depends critically on the above-mentioned spectroscopic and thermo-optical parameters. In addition, with the present approach additional parameter such as pump quantum efficiency, effect of ESA on the laser emission, etc were obtained.

Acknowledgements

The authors are thankful to Brazilian agencies CNPq, FAPESP, CAPES, and FAPESP, and Comunidad Autónoma de Madrid (project CCCG07-UAM/MAT-1861) and Spanish Ministerio de Ciencia y Tecnología (MAT2007-64686) for the financial support of this work.